Gondwana Research 15 (2009) 267–275

Contents lists available at ScienceDirect

Gondwana Research

journal homepage: www.elsevier.com/locate/gr

Supercontinent formation from stochastic collision and mantle convection models

Nan Zhang [a,*], Shijie Zhong [a], Allen K. McNarmara [b]

[a] Department of Physics, University of Colorado, Boulder, CO 80309, USA
[b] School of Earth and Space Exploration, Arizona State University, Tempe, AZ 85287, USA

ARTICLE INFO

Article history:
Received 19 July 2008
Received in revised form 18 October 2008
Accepted 19 October 2008
Available online 30 October 2008

Keywords:
Supercontinent formation
Stochastic collision model
Mantle convection model

ABSTRACT

The large-scale tectonics in the last billion years (Ga) are predominated by the assembly and breakup of supercontinents Rodinia and Pangea. The mechanisms controlling the assembly of supercontinents are not clear. Here, we investigate the assembly of a supercontinent with 1) stochastic models of randomly-moving continental blocks and 2) 3-D spherical models of mantle convection with continental blocks. For the stochastic models, we determined the time required for all the blocks to assemble into a single supercontinent on a spherical surface. We found that the assembly time from our stochastic models is significantly longer than inferred for Pangea and Rodinia. However, our study also suggests that the assembly time from stochastic models is sensitive to the rules for randomly assigning continental motion in the models. In our dynamic models of mantle convection, continental blocks are modeled as deformable and compositionally distinct materials from the mantle. We found that mantle convective planform has significant effects on supercontinent assembly. For models with moderately strong lithosphere and the lower mantle relative to the upper mantle that lead to degree-1 mantle convection, continental blocks always assemble to a supercontinent in ~250 million years (Ma) and this assembly time is consistent with inferred for Pangea and Rodinia. However, for models with intrinsically small-scale mantle flows, we found that even when continental blocks merge to form a supercontinent, the assembly times are too long and the convective structures outside of supercontinent regions are of too small wavelengths, compared with observed.

1. Introduction

The assembly and breakup of supercontinents are fundamental processes that affect the Earth's geological evolution and control the large-scale tectonics including the mountain building and seafloor spreading (see Murphy et al., 2009-this issue; Eriksson et al., 2009-this issue; Santosh et al., 2009-this issue). Recent reconstructions of continental motions and supercontinents suggest that time scales for supercontinent cycles are ~600 Ma with a life time of ~150 Ma for a supercontinent and 400–450 Ma for supercontinent breakup and assembly (Hoffman, 1991; Torsvik, 2003; Li et al., 2008). A Paleo-Mesoproterozoic supercontinent Columbia has been proposed to exist until 1.5 Ga ago (Rogers and Santosh, 2002; Rogers and Santosh, 2009-this issue). After the breakup of Columbia, the dispersed continental blocks accreted around the margin of Laurentia and formed supercontinent Rodinia 900 Ma ago (Weil et al., 1998; Tosvik, 2003; Li et al., 2004; Li et al., 2008; Rino et al., 2008). Rodinia existed for ~150 Ma and started to breakup at ~750 Ma ago. The most recent supercontinent Pangea formed around 320 Ma ago as Gondwana and Laurussia collided near the equator (Smith et al., 1981; Veevers, 2004). Similar to Rodinia, Pangea existed for ~150 Ma and started to breakup ~175 Ma ago.

Supercontinent processes have implications for the present-day mantle structure. Seismic tomography models (Su and Dziewonski, 1997; van der Hilst et al., 1997; Ritsema et al., 1999; Masters et al., 2000; Grand, 2002; Romanowicz and Gung, 2002) have showed that the present-day mantle is predominated by degree-2 structure with two major seismically low velocity anomalies beneath Africa and the mid-Pacific that are surrounded by circum-Pacific seismically fast anomalies. The African seismic anomaly is located where Pangea was and is suggested to be related to Pangea (Anderson, 1982; Hager et al., 1985). Circum-Pacific seismic anomalies are related to the subduction history of last 120 Ma (Hager et al., 1985; Lithgow-Bertelloni and Richards, 1998; Maruyama et al., 2007; see also Zhao, 2009-this issue) which is related to the previous subduction around Pangea (e.g., Scotese, 1997). The Pacific anomaly, which is antipodal to the African anomaly, is suggested to play an important role in forming Pangea (Zhong et al., 2007). Therefore, the present-day mantle structure may be closely related to Pangea.

Supercontinent processes may also have important implications for the dynamics of the mantle (Anderson, 1982; Gurnis, 1998; also see Ernst, 2009-this issue; Coltice et al., 2009-this issue). Both Pangea and Rodinia were surrounded by subduction zones (Scotese, 1997; Torsvik, 2003; Li et al., 2008). Before and during their breakup, Pangea and Rodinia experienced large-scale rifting, volcanism and magmatism (Hoffman, 1991; Li et al., 2008). It has been suggested that the volcanism and supercontinent breakup are caused by the thermal

* Corresponding author.
E-mail address: nan.zhang@colorado.edu (N. Zhang).

1342-937X/$ – see front matter © 2008 International Association for Gondwana Research. Published by Elsevier B.V. All rights reserved.
doi:10.1016/j.gr.2008.10.002

insulation effects of a supercontinent (Anderson, 1982; Gurnis, 1998). However, recent numerical modeling of supercontinent processes in three-dimensional spherical models suggests that return flows induced by circum-supercontinent subduction may play a more important role in causing the volcanism and supercontinent breakup (Zhong et al., 2007), consistent with previous two-dimensional modeling studies (Gurnis, 1998; Lowman and Jarvis, 1995). This is also supported by the inference that with the relatively small radiogenic heating in the depleted upper mantle, the thermal insulation effect is rather weak in the relatively short life times of supercontinents (Korenaga, 2007; Zhong et al., 2007).

The processes responsible for supercontinent assembly are more controversial with two competing proposals. First, it has been suggested that a supercontinent may be formed as a result of collision of randomly moving continents with no explicit involvement of the underlying mantle (Tao and Jarvis, 2002). Modeling the collision of randomly moving continents using rule-based stochastic models suggested that such a mechanism can lead to formation of a supercontinent on time-scales of 400 Ma, consistent with that observed. Second, the formation of supercontinents is considered as a consequence of mantle dynamics (Lowman and Jarvis, 1995; Gurnis, 1998; Phillips and Bunge, 2005, 2007). Using 2-D mantle convection models, Gurnis (1998) showed that continental blocks merge above downwellings to form a supercontinent, a result that is later confirmed by other 2-D (Lowman and Jarvis, 1995) or 3-D (Phillips and Bunge, 2005, 2007) models. Phillips and Bunge (2007) examined the effects of various convection parameters including internal heating on the period of supercontinent cycles.

However, a relevant question that was not explicitly addressed in these dynamic models is the control of convective planform on supercontinent formation. Can a supercontinent be formed in a mantle with small-scale convective structures and multiple downwellings? If so, this may provide a physical basis for the stochastic model of Tao and Jarvis (2002) with randomly moving continental blocks, given that small-scale structures may not affect continental motions in a coherent way. Alternatively, does supercontinent formation require long-wavelength flow structure? How are the long-wavelength structures for supercontinent formation related to the present-day mantle structures?

Some of these questions were answered in a recent study by Zhong et al. (2007). In a 3-D spherical model of mantle convection, Zhong et al. (2007) showed that with relatively realistic mantle viscosity (i.e., moderately high viscosities for both lithosphere and lower mantle, relative to the upper mantle), mantle convection is characterized by a degree-1 planform in which one hemisphere is dominated by downwellings while the other by upwellings. They suggest that such a degree-1 convection causes continental blocks to merge in the downwelling hemisphere to form a supercontinent. They further showed that after a supercontinent is formed in the downwelling hemisphere, circum-supercontinent subduction induces another major upwelling system below the supercontinent, transforming the degree-1 planform to degree-2 planform with two antipodal upwellings. Zhong et al. (2007) suggested that this transition between degree-1 and degree-2 planforms of mantle convection modulated by continents is essential for supercontinent processes, and that the present-day mantle with degree-2 structure and two antipodal superplumes (African and Pacific) reflects the aftermath of Pangea breakup. This proposal is different from an early suggestion by Evans (2003) that a supercontinent is formed in a downwelling girdle separating two major upwellings in a mantle with largely degree-2 structure.

The main goals of this study are to continue exploring these two proposed models for supercontinent formation, i.e. the stochastic models for collision of randomly-moving continents and dynamic models of continental motions driven by mantle convection. We intend to answer the following specific questions. For stochastic models with randomly moving continents in which the dynamics of the mantle are left out, how are the time-scales for supercontinent formation dependent on different rules (e.g., Tao and Jarvis, 2002)? For dynamic models of continental motions driven by mantle convection, how does supercontinent formation depend on planform of mantle convection? Can a supercontinent form in mantle convection dominated by small-scale flow structures? If so, what is the time-scale for its formation? Our dynamic models of supercontinent formation in 3-D spherical convection models with multiple mobile continents represent a significant improvement compared with Zhong et al. (2007) in which either no continent or only one fixed continent was considered. Our studies also differ from Phillips and Bunge (2005, 2007) in which continental blocks are modeled as rigid, non-deformable blocks using the torque balance technique (Gable et al., 1991). In our study, continents are modeled as compositionally distinct and deformable (Zhong et al., 2000; McNamara and Zhong, 2004), similar to what was done in previous 2-D models (Lenardic and Kaula, 1993; Lenardic and Moresi, 1999). Additionally, our study emphasizes the role of convective planform in supercontinent formation, while Phillips and Bunge's studies were focused on the role of internal heating in the periods of supercontinent cycles.

This paper is organized as follows. Section 2 describes the models and methods. In which we present 1) our algorithms for models with randomly-moving continental blocks and 2) mathematical formulations and models of mantle convection with continents. Section 3 presents model results. Discussions and conclusions are presented in Sections Section 4 and 5.

2. Models and methods

2.1. The rule-based model with randomly-moving continental blocks

In order to explore the assembly time of randomly-moving continental blocks, following Tao and Jarvis (2002), we employ a stochastic model and monitor the time required for all of continental blocks to assemble into a single model supercontinent. We first describe our models, and then discuss the difference between ours and Tao and Jarvis's model.

In our model, n circular blocks are initially evenly or randomly distributed on a spherical surface, and the total area of the blocks accounts for 30% of the spherical surface. Initially, each block is randomly assigned an Euler pole, and the angular speed for all the blocks are the same. At each time step, the speed for each block is varied randomly within a certain range (50%) of the initially specified speed.

The model evolves according to the following rules:

(1) Any two blocks are considered merged if the distance between the centers of the two blocks is less than 2/3 of the sum of radii of these two blocks. If at a given step, more than two blocks collide, only the two blocks with the shortest distance between the centers merge.
(2) Once two blocks are considered merged, they are replaced with a new circular block. The center of the new block is the middle point between the centers of the previous two blocks and its area is the sum of the previous blocks.
(3) A new Euler pole is assigned randomly to the new block and the new block moves on until the next collision.
(4) When all the blocks merge into a single super-block, we count the number of time steps the assembling process takes and obtain the assembly time. In order to obtain the statistical average of assembly time, we repeat the above model calculation 10,000 times and then compute the average assembly time for these 10,000 runs.

In this model, the speed and the initial number of continental blocks may influence the assembly time. To examine their effects, the speed is varied from 1 cm/yr to 15 cm/yr and the initial number of continental blocks is varied from 4 to 12.

A different set of rules was used by Tao and Jarvis (2002) in their model with randomly-moving continental blocks. In their model, circular blocks are on a Cartesian plane with periodic boundary condition. They assigned random initial velocities with a plate-like range from one to ten cm/yr. They updated the random velocities every 50 Ma and assigned a new velocity direction for a block randomly within $\pm 45°$ of previous direction. In this study, we also implemented the rules used in Tao and Jarvis (2002), and compared results from our models to examine the effects of different rules on assembly time.

2.2. Mantle convection models with continents

Our dynamic models of mantle convection with continental blocks in a three-dimensional spherical geometry assume an infinite Prandtl number and the Boussinesq approximation. Continental blocks are modeled as a chemical distinct material with different density and viscosity. The non-dimensional governing equations for mantle convection with different compositions are (e.g., Zhong et al., 2000; McNamara and Zhong, 2004):

$$\nabla \cdot \mathbf{u} = 0 \tag{1}$$

$$-\nabla P + \nabla \cdot (\eta \dot{\varepsilon}) = (RaT - RbC)\hat{e}_r, \tag{2}$$

$$\frac{\partial T}{\partial t} + \left(\mathbf{u} \cdot \nabla\right)\mathrm{T} = \nabla^2 \mathrm{T} + \mathrm{H}, \tag{3}$$

$$\frac{\partial C}{\partial t} + (\mathbf{u} \cdot \nabla)\mathrm{C} = 0, \tag{4}$$

where $\mathbf{u}$ is velocity vector, P is the dynamic pressure, η is the viscosity, $\dot{\varepsilon}$ is the strain rate tensor, T is the temperature, t is the time, H is internal heat generation rate, and C is the composition that is used to define continental blocks.

Ra is the thermal Rayleigh number defined as

$$Ra = \alpha \rho g \Delta T R_0^3 / (\eta_r \kappa), \tag{5}$$

where α is the thermal expansivity, ρ is the density, g is the gravitational acceleration, ΔT is the temperature difference between the top and bottom boundaries, R_0 is the radius of the Earth, η_r is the reference viscosity, and κ is the thermal diffusivity. Notice that if Ra is defined by mantle thickness, d, a conversion factor, $(d/R_0)^3$, needs to be multiplied (Zhong et al., 2000).

Internal heat generation rate H is defined as

$$H = \frac{QR_0^2}{\rho c_p \kappa \Delta T}, \tag{6}$$

where Q is the volumetric heat production rate, and c_p is the specific heat.

Rb is the chemical Rayleigh number defined as

$$Rb = g \Delta \rho R_0^3 / (\eta_r \kappa), \tag{7}$$

where $\Delta\rho$ is the density contrast between two chemical components (e.g., continents versus the mantle). A useful parameter is the buoyancy ratio, B

$$B = Rb / Ra = \Delta\rho / (\alpha \rho \Delta T). \tag{8}$$

The nondimensional depth-, temperature-, and composition-dependent viscosity is

$$\eta(T, C) = \eta_0(r)\eta_c exp[E(0.5 - T)], \tag{9}$$

where η_0 is the depth dependent prefactor, η_c is the compositional prefactor, and E is the activation energy.

The nondimensional radii for the top and bottom boundaries are 1 and 0.55, respectively. Free-slip and isothermal boundary conditions are applied at the surface and the core–mantle boundary in all calculations. Therefore, continental blocks are free to move and deform to interact with mantle flows.

The governing equations are solved with code CitcomS (Zhong et al., 2000) that was modified from an original Cartesian code (Moresi and Gurnis, 1996). Thermochemical convection capability was incorporated into CitcomS by McNamara and Zhong (2004). The mantle is divided into 12 caps and each cap is further divided into 48 elements in three directions. Our previous calculations show that resolution is adequate for this type of calculation (Zhong et al., 2007).

Our models include six model parameters: thermal Rayleigh number Ra, depth-dependent viscosity prefactor $\eta_0(r)$, internal heat generation rate H, activation energy E, buoyancy ratio B, and compositional prefactor η_c. The last two parameters B and η_c are used to describe continental blocks. To maintain the integrity for continents and minimize the chemical entrainment for continental materials during model calculations, B and η_c are set to be 0.5 and 200, respectively for all calculations with continents. Too high η_c may introduce numerical convergence difficulty when continental blocks collide, while too small η_c may lead to too large deformation and entrainment. We fix activation energy E to be 6.908 that gives rise to 10^3 viscosity variation for the temperature varying from 0 to 1. With this activation energy, our model captures the essential features of mantle convection with temperature-dependent viscosity, and mantle convection remains in the mobile-lid regime (e.g., Solomatov, 1995). We also fix internal heat generation rate H and thermal Rayleigh number Ra in our models, while varying $\eta_0(r)$ to explore the effects of convective planform. With temperature-dependent viscosity and the free-slip boundary condition on the surface, our models are not able to reproduce plate-like behaviors for oceanic regions, although the temperature-dependent viscosity generates the long-wavelength convective structures. Convection models with plate tectonics require more realistic modeling of the nonlinear or plastic deformation of lithosphere at plate margins, which remains a challenge in mantle dynamics (e.g., Bercovici, 1995; Zhong et al., 1998; Tackley, 2000).

Calculations are performed in two steps. Firstly, for a given set of parameters, a pure thermal convection model is computed until global

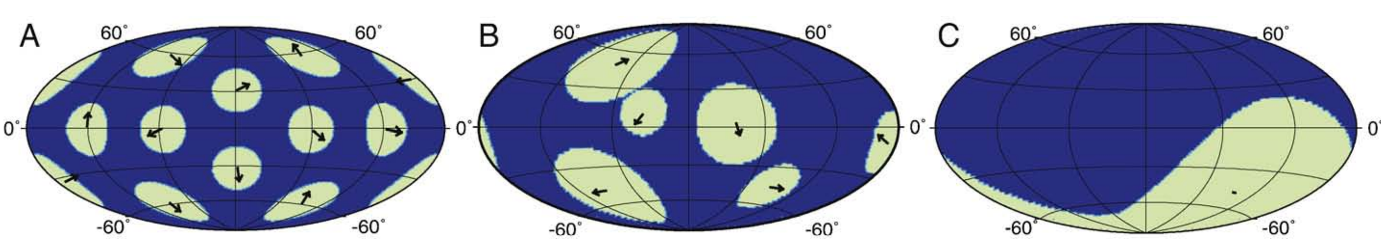

Fig. 1. Locations of continents at three different times in a representative model calculation for the stochastic models of continental collision. The initially 12 continents (A) merge to six continents (B), and eventually form a supercontinent (C). The arrows give the directions of continental motions.

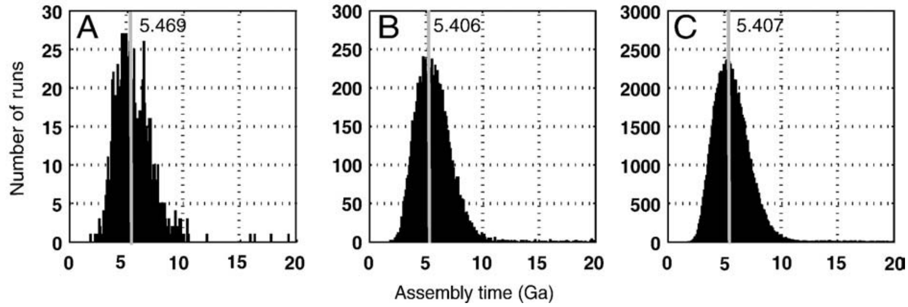

Fig. 2. Histograms of assembly times for 1000 runs (A), 10,000 runs (B), and 100,000 runs (C) of stochastic models with 1 cm/yr speed. The averaged assembly times (the vertical bar) are 5469 Ma for 1000 runs, 5406 Ma for 10,000 runs and 5407 Ma for 100,000 runs, respectively.

average quantities (e.g., heat flux and root mean square velocity) reach to a statistic steady-state. Initial temperature conditions of the purely thermal convection models consist of a radial temperature profile superimposed with horizontal perturbations. The initial temperature is 0.5 for the mantle interior and changes linearly to boundary temperatures 0 or 1 across the top or bottom thermal boundary layers. Secondly, for the same model parameters, using the steady-state temperature field from these purely thermal convection models as initial conditions (Honda et al., 2000; Phillips and Bunge, 2007), a certain number of continental blocks are introduced in model calculations to examine the dynamic interaction between convection and continents. For models with continental blocks, we introduce either two or four continental blocks with total continental area accounting for 30% of the Earth's surface. The thicknesses of continental blocks are set to be 100 km. In these models, we trace the motion and collision of continental blocks and investigate the role of mantle convection in the assembly of continental blocks.

3. Results

In this section, we first present results from our stochastic models with randomly-moving continental blocks and compare our model results with those from Tao and Jarvis (2002). We will then present results from dynamic models of mantle convection with continental blocks.

3.1. Assembly time of the randomly-moving blocks

3.1.1. The assembly process and the statistic average for the assembly time

We first present a case with initial continental motion of 1 cm/yr to show the assembly process of randomly moving blocks (Fig. 1). This case has initially 12 continental blocks each with a surface area equal to 2.5% of the area of the spherical surface. Fig. 1 shows three snapshots of positions and sizes of continental blocks from the assembly process. In this case, initially 12 continental blocks merge to six blocks of different sizes after 1400 Ma (Fig. 1B). They assemble to a supercontinent after 5380 Ma (Fig. 1C).

A large number of runs are needed in order to obtain a statistically meaningful average assembly time. For the same initial number of blocks and average speed of continental motion, we have computed 1,000, 10,000, and 100,000 model runs and three histograms showing the frequency distribution of assembly times are plotted in Fig. 2. These results show that 10,000 runs are sufficient for obtaining a stable statistic average of assembly time, which is ~5.4 Ga for this model.

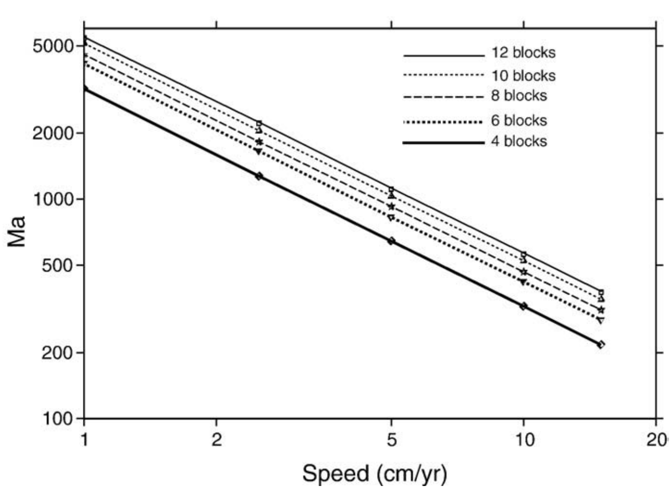

Fig. 3. The inversely proportional relation between the assembly times and the average continental speeds for stochastic models with initially 4 (diamond symbols), 6 (inverted triangles), 8 (stars), 10 (triangles), and 12 (squares) continents. Each symbol represents averaged assembly time from 10,000 runs.

3.1.2. Dependence of assembly time on continental motion and number of blocks

Assembly time may depend on the average speed of continental blocks and initial number of blocks. For a fixed initial number of blocks, we compute models with average speed of 1 cm/yr, 2.5 cm/yr, 5 cm/yr, 10 cm/yr and 15 cm/yr and determine the average assembly times (Fig. 3). It should be noted that each assembly time in Fig. 3 is obtained from 10,000 runs for a given initial number of blocks and average speed. For a given initial number of blocks, the assembly time is inversely proportional to the average block speed (Fig. 3). Therefore, we only show results of assembly times for continental blocks with average speed of 1 cm/yr in Table 1. For different average speeds, one can easily obtain assembly time by scaling the results in Table 1.

Our model calculations show that the assembly times are moderately dependent on the initial number of blocks (Table 1 and Fig. 3). If we employ the averaged speed for present-day continents, 2.8 cm/yr, which is calculated based on the NUVEL-1 model in a Non-Net-Rotation frame (Gordon and Jurdy, 1996) and weighed by continental area, the results in Table 1 suggest that assembly time varies from 1200 Ma for initially four blocks to 1900 Ma for initially 12 blocks. This is significantly longer than the observed assembly time for supercontinent which is ~300–400 Ma.

3.1.3. The comparisons between our model and Tao and Jarvis' model (2002)

In a similar study, Tao and Jarvis (2002) employed a different set of rules for the assembly process and suggested a different assembly time (~400 Ma) of randomly-moving continental blocks.

To investigate the cause for the difference on the predicted assembly times between our models and Tao and Jarvis (2002), we first implemented their models in Cartisian geometry and reproduced their

Table 1
The assembly times determined from the stochastic models[a].

Number of blocks	12	10	8	6	4
Assembly time (Ma)	5407	5103	4610	4120	3220

[a] All the calculations use 1 cm/yr as the speed of continental motion.

Table 2
Input parameters and assembly times for dynamic models of mantle convection.

Case	$\eta_{0\ \mathrm{um}}$ [a]	I.C.[b] (l,m)	n[c]	Strongest degree (s)[d]	Assembly times (Ma)[e]	Surface velocity	ξ (%)[f]
1	1	(3,2)	–	6,9	–	2.612×10^3	41
1A	1	Case 1	2	2,4	–	2.638×10^3	47
1B	1	Case 1	4	1,2,6	650	3.201×10^3	49
1C	1/30	Case 1	4	1	270	8.915×10^3	37
2	1/3	(3,2)	–	3,4	–	3.782×10^3	36
2A	1/3	Case 2	2	1,2,3,4	505	5.250×10^3	42
2B	1/3	Case 2	4	1,2,3	365	4.159×10^3	43
2C	1/30	Case 2	4	1	260	7.585×10^3	32

[a] $\eta_{0\ \mathrm{um}}$ is the pre-exponential factor for the viscosity equation for the top 100 km and between 100 km and 670 km depths. η_0 for the lower mantle is 1.
[b] I.C. is the initial conditions. For pure thermal case 1 or 2, the initial condition is perturbation at some given spherical harmonic degree l and m. For thermochemical cases, the initial conditions are from the stable thermal structures of case 1 or 2.
[c] n is the number of continental blocks.
[d] Strongest degrees are the dominant spherical harmonic degrees of temperature fields after the steady-state is reached or the supercontinents are formed.
[e] Assembly times are measured in terms of transit times.
[f] ξ is the internal heating rate.

models D-7 and D-20. Then, we introduced Tao and Jarvis' rules to our spherical model to investigate the dependence of assembly time on different rules. For better comparison, we also assumed that model continents account for 35% of the Earth's surface, employed continental motion speed from one to ten cm/yr, and let the continents on the spherical surface randomly moving along great circles instead of randomly assigning Euler poles.

With the rules by Tao and Jarvis (2002) in our spherical model, we obtain the assembly times 280 Ma with initially seven blocks (i.e., corresponding Tao and Jarvis' model D-7) and 354 Ma with initially 20 circles (i.e., corresponding Tao and Jarvis' model D-20), which are similar to Tao and Jarvis (2002), suggesting that the geometry effect is small. If we replaced their rule assigning a new velocity direction after an interval of 50 Ma with our original rule assigning a new velocity after a collision, the assembly times increase from 280 Ma to 997 Ma for initially seven blocks and 354 Ma to 1281 Ma for initially 20 blocks, respectively. If we further replaced the rule limiting velocity direction within ±45° of its previous direction with our rule of all the possible directions in assigning to continents after collision (i.e., 360 degrees), the assembly time increases from 997 Ma to 1541 Ma for initially seven blocks and 1281 Ma to 2542 Ma for initially 20 blocks. In this case, the model is essentially the same as our original model, and the assembly times are of the same magnitude as that from our models in subsection 3.1.2. This result suggests that the assembly time is sensitive to the rules for assigning the random velocity, which suggests the importance of dynamic models of mantle convection.

3.2. Supercontinent formations in dynamic models of mantle convection

3.2.1. Models of mantle convection with no continents

We first present two cases with no continental blocks to be used as initial temperature conditions for later cases with continents. Case 1 uses a Rayleigh number $Ra=3\times10^8$ (i.e., $Ra=2.73\times10^7$ if the mantle thickness is used to define Ra), internal heat generation rate $H=50$, and a constant depth-dependent viscosity prefactor $\eta_0(r)=1$ throughout the mantle (Table 2). The initial temperature has a perturbation at spherical harmonic degree $l=3$ and $m=2$. The viscosity profile of case 1 is shown in Fig. 4A. We compute the case for ~30,000 time steps to a statistical steady-state. The representative planform of mantle convection is characterized by relatively short-wavelengths with a large number of upwellings and downwellings in the mantle (Figs. 5A and 6A). Power spectra for temperature within the bottom thermal boundary layer display a maximum amplitude at degrees 6 and 9 (Fig. 4B). The averaged surface velocity at the steady-state is ~2.6×10^3 (Table 2). The internal heating rate, determined from the averaged surface and bottom heat flux, is 41% (Table 2).

Case 2 differs from Case 1 only in having a reduced upper mantle viscosity with $\eta_0(r)=1/3$ between 100 km and 670 km depths and $\eta_0(r)=1$ elsewhere (Table 2). The viscosity profile of case 2 is shown in Fig. 4A. We compute case 2 for ~40,000 time steps to a statistical steady-state. Although case 2, similar to case 1, has a large number of upwellings and downwellings in the mantle (Figs. 5B and 6B), convective wavelengths for case 2 are increased compared to case 1 (Fig. 5A), reflecting the effect of weak upper mantle on convective wavelengths (Jaupart and Parson, 1985; Bunge et al., 1996; Zhong et al., 2007).

3.2.2. Supercontinent formation in convection with small-scale thermal structures

Case 1A uses the same parameters as case 1, but includes two continental blocks. Case 1A uses the steady-state temperature field from case 1 (i.e., Figs. 5A and 6A) as initial conditions. One continental block is initially assigned with a random position, while the other continental block is antipodal to it. The viscosity profile of case 1A is similar to that from case 1 as shown in Fig. 4 except that the viscosity at the top is larger due to the compositional viscosity for continents. Following Zhong and Gurnis (1993), we use transit time to measure times and to compare with the observation time-scale. A transit time is defined as the time it takes a flow particle to travel at the averaged speed at the surface from the surface to the core–mantle boundary. On the Earth, one transit time is ~50 Ma, taking the averaged surface plate motion to be ~6 cm/yr.

For case 1A, after six transit times corresponding to ~300 Ma, the large-scale cold anomalies have accumulated around these two continental blocks but only at shallow depths (Fig. 7B). After 17 transit times (i.e., 850 Ma), these two blocks are still wandering around with no indication of merging to a supercontinent (Figs. 6C and 7C), and we

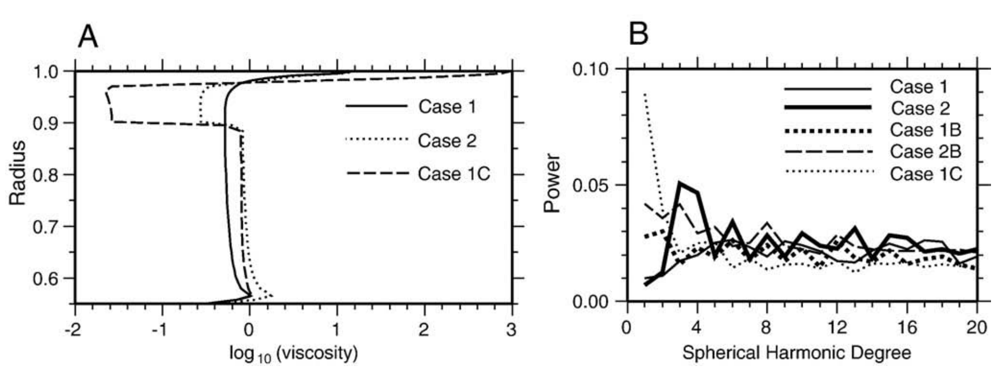

Fig. 4. The depth-dependences of horizontally averaged mantle viscosities for cases 1, 2, and 1C (A), and power spectra of temperature within the bottom thermal boundary layers for cases 1, 2, 1B, 2B, and 1C (B). The spectra for cases 1 and 2 are steady-state results, while the spectra for cases 1B, 2B, and 1C are for that after the assembly of supercontinents.

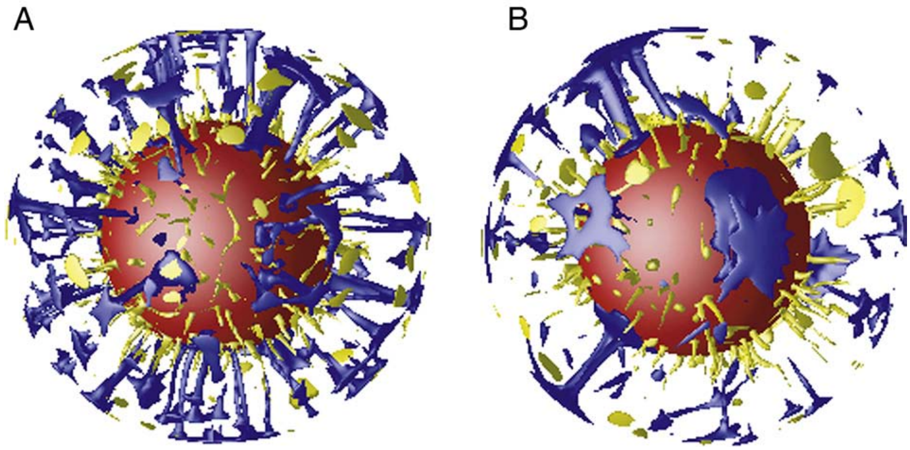

Fig. 5. Three dimensional thermal structures for cases 1 (A) and 2 (B) at their statistically steady states. The thermal structures are plotted as isosurfaces of residual temperature with contour levels of −0.15 (blue) and 0.15 (yellow). (For interpretation of the references to color in this figure legend, the reader is referred to the web version of this article.)

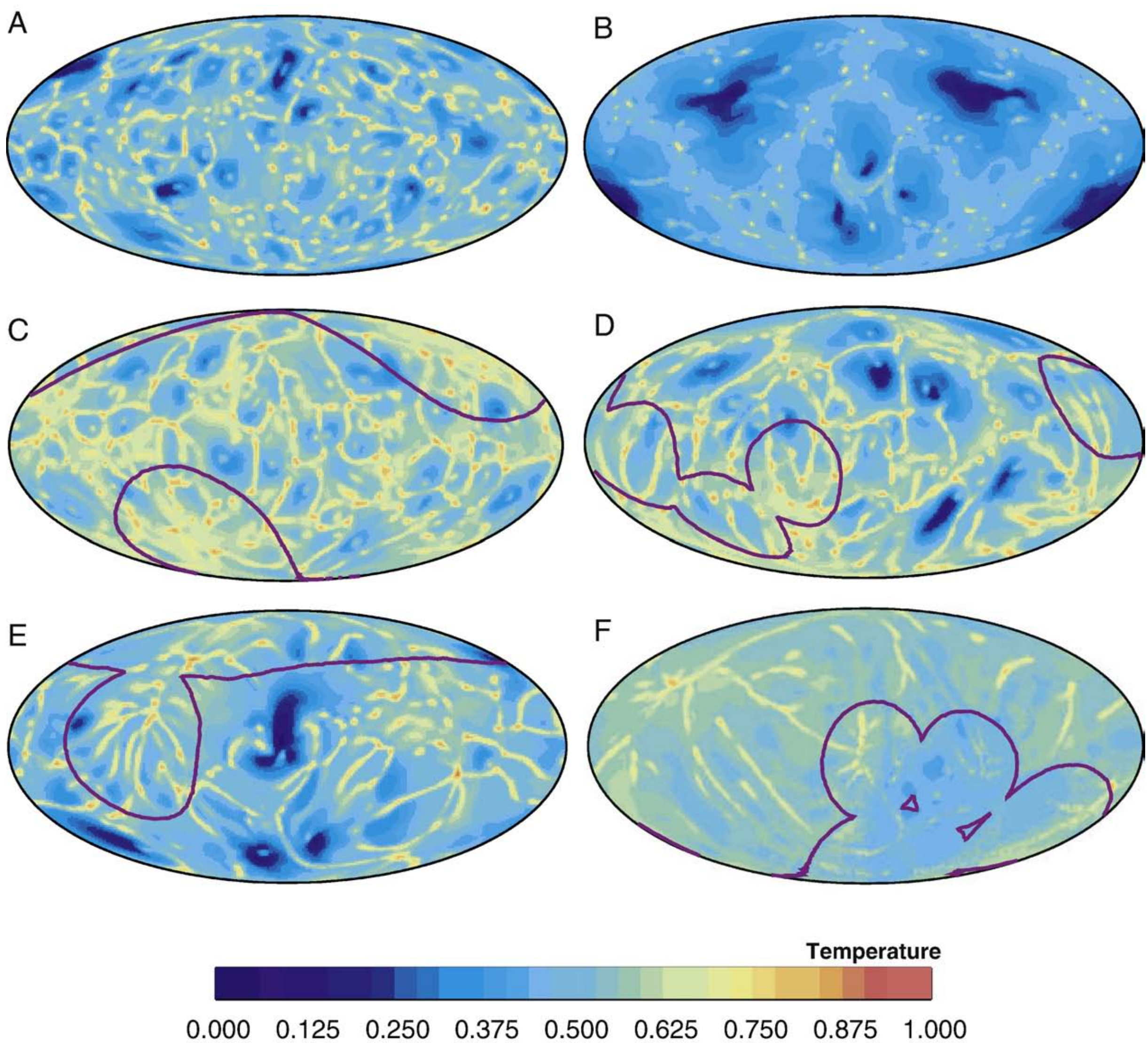

Fig. 6. Temperature fields at non-dimensional radius 0.59 for cases 1 (A), 2 (B), 1A (C), 1B (D), 2A (E), and 1C (F). Purple curves in (C), (D), (E), and (F) delineate the boundaries of continents. (For interpretation of the references to color in this figure legend, the reader is referred to the web version of this article.)

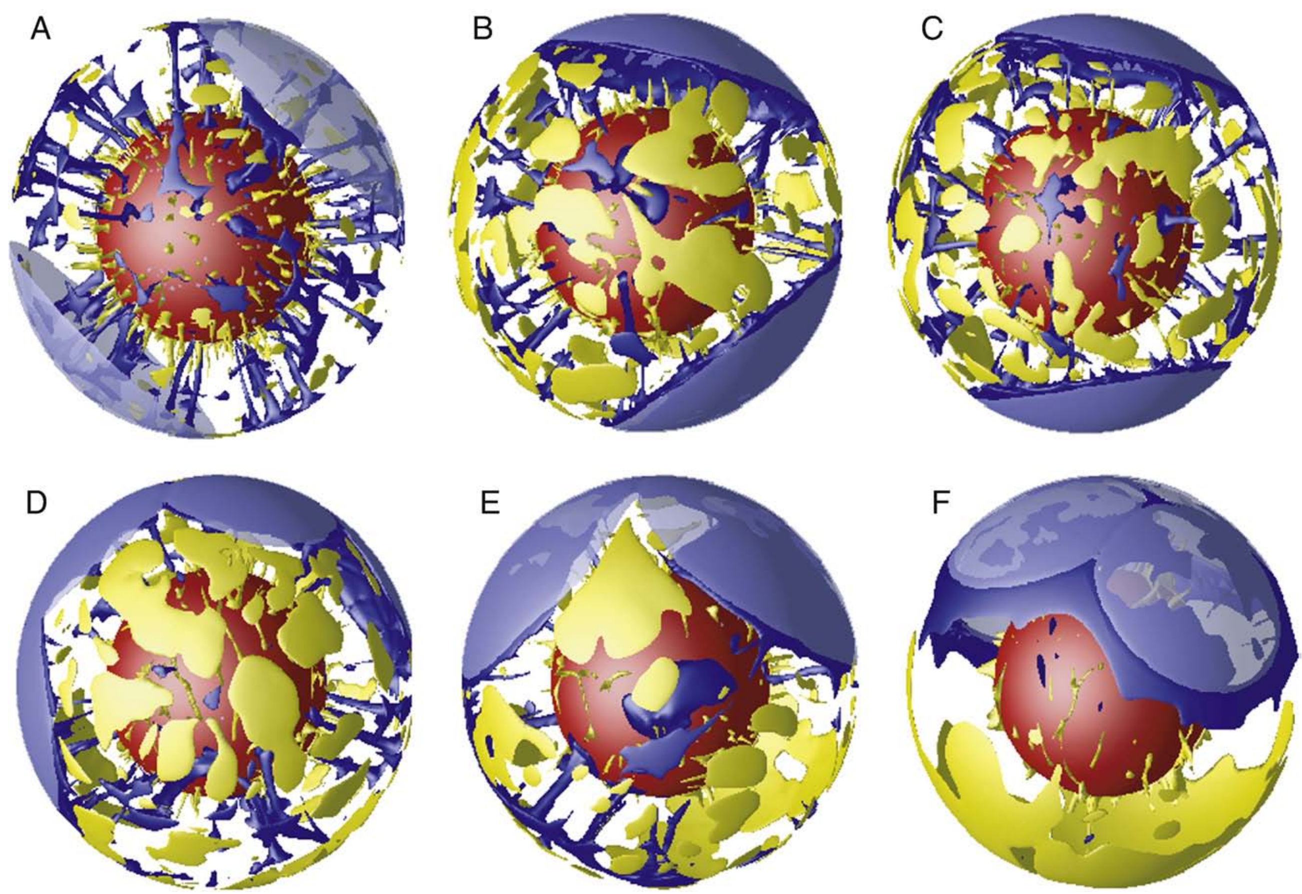

Fig. 7. Thermal structures and locations of continents (transparent caps) for cases 1A at its initial stage (A), after six (B) and 17 transit times (C), 1B (D), 2A (E), and 1C (F) at supercontinent formation. The thermal structures are plotted as isosurfaces of residual temperature with contour levels of −0.15 (blue) and 0.15 (yellow). Notice that the thermal structures in A is the same as that in Fig. 5A but with a different orientation. (For interpretation of the references to color in this figure legend, the reader is referred to the web version of this article.)

terminate this case at this point. This case indicates that mantle convection with small-scale structures may not lead to supercontinent formation.

Case 1B differs from Case 1A only in having four continental blocks instead of two. One continental block is initially assigned with a random position on the surface. Then other three blocks are assigned to the positions to form a tetrahedron with the first block. After 13 transit times (i.e., ~650 Ma), all of four blocks have merged to a supercontinent (Figs. 6D and 7D). Long-wavelength structures including linear downwellings are generated around the supercontinent (Fig. 7D). The power spectrum of the thermal structures in the bottom thermal boundary shows the strongest amplitude at degree 2 (Fig. 4B), consistent with the increased convective wavelengths seen in Fig. 7D, compared to case 1. This increased wavelength reflects the effects of supercontinent (Zhong and Gurnis, 1993). However, it is important to observe that the thermal structures outside of the supercontinent region are of relatively small-scale wavelengths with a large number of downwellings and upwellings (Fig. 6D), similar to that in case 1.

Using the steady-state thermal structure for case 2 (Figs. 5B and 6B) as initial conditions, we computed cases 2A and 2B that initially include two and four continental blocks, respectively. Cases 2A and 2B are identical to case 2, except for including continental blocks. Compared with cases 1A and 1B, the upper mantle viscosity is reduced by a factor of three in cases 2A and 2B. For case 2A, the two continental blocks merge to a supercontinent after 10.1 transit times corresponding to 505 Ma (Fig. 7E). In case 2B, all four continental blocks merge to form a supercontinent after ~7.3 transit times or ~365 Ma. Similar to what was observed in cases 1A and 1B, while supercontinents introduce long-wavelength structures near them, regions outside of supercontinents are predominated by shorter-wavelength structures in the form of downwellings and upwellings (Figs. 6E and 7E). However, relative to cases 1A and 1B, cases 2A and 2B with reduced viscosity in the upper mantle, appear to have large convective wavelengths in non-continental regions (Figs. 6E and 7E), similar to what has been observed for cases 1 and 2.

3.2.3. Supercontinent formation in mantle convection with long-wavelength structures

Zhong et al. (2007) found that with a weak upper mantle bounded by relatively strong lithosphere and lower mantle, mantle convection is characterized by very long wavelength (i.e., degree-1) planform that they suggested to be responsible for supercontinent formation. Here, we explore the models with the same viscosity structure used in Zhong et al. (2007) (i.e., $\eta_0(r) = 1/30$ between the depths of 100 km and 670 km, while it is unity elsewhere) but with continental blocks to investigate the supercontinent formation. We have calculated cases 1C and 2C that differ only in using different initial conditions, otherwise they are identical (Table 2). Case 1C uses the steady-state temperature from case 1 (Fig. 5A), while case 2C uses that from case 2 (Fig. 5B). Both cases 1C and 2C use the viscosity with a factor of 30 reduction in the upper mantle (Fig. 4A) and include four continental blocks in their initial setup. For case 1C, after 5.4 transit times (i.e., ~270 Ma), all four continental blocks merge to form a supercontinent (Figs. 6F and 7F). The thermal structure evolves to a degree one pattern (Fig. 6F). The spectrum of the thermal structures after the supercontinent formation is shown in Fig. 4B. Clearly, the degree-1 pattern dominates the convection at the late stage. The results from case 2C are essentially the same as for case 1C with a slight different assembly time at ~260 Ma, suggesting that the results are insensitive to initial conditions.

4. Discussion

Among the studies on the mechanism and cause for supercontinent formation (Lowman and Jarvis, 1993, 1995; Gurnis, 1998; Phillips and Bunge, 2007), there are two end-member views. First, Zhong et al. (2007) found that mantle convection with moderately strong lithosphere and lower mantle than the upper mantle always evolves to a degree-1 planform and suggested that such a degree-1 planform plays an important role in causing supercontinents Pangea and Rodinia. Second, Tao and Jarvis (2002), from their stochastic models for randomly moving continents, suggested that supercontinent formation may result from collision of randomly moving continents at time-scales of ~400 Ma for the formation process with no explicit role of mantle convective structures.

The current study found that the time-scale for supercontinent formation from the stochastic models depends greatly on the rules assumed in the models. While reproducing their ~400 Ma time-scales of supercontinent formation using similar rules as Tao and Jarvis (2002), we also found that using different but arguably equally plausible rules, the time-scales for supercontinent formation can be significantly longer at 1 Ga or longer. Therefore, we think that it is important to study the physics and dynamics of supercontinent formation and mantle convection and to understand the rules (Lowman and Jarvis, 1993, 1995; Gurnis, 1998; Phillips and Bunge, 2007). This is further supported by our dynamic models of mantle convection with continents. In some of such dynamic models, continental blocks may never merge to a supercontinent in mantle convection predominated by small-scale structures (e.g., Case 1A). In other dynamic models, while continental blocks merge to form a supercontinent in convection with intrinsically small-scale structures, the assembly times may be too long and the convective structures outside of supercontinent regions are of too small wavelengths to be consistent with geological and geophysical observations (e.g., Cases 1B, 2A and 2B).

Our study also supports the proposal by Zhong et al. (2007) on the importance of very long-wavelength mantle convection. Using similar viscosity structure as in Zhong et al. (2007), we find that starting from a small-scale convective planform, a supercontinent always forms on a time-scale of ~260 Ma. Additionally, during the supercontinent assembly process, mantle convection is predominated by degree-1 planform, consistent with Zhong et al. (2007). Although the inferred non-supercontinent period for Pangea and Rodinia is ~400 Ma as reviewed in the Introduction, we think that this is not inconsistent with our ~260 Ma supercontinent formation time-scales. This is because that after supercontinent breakup starts, it may last for more than 100 Ma with a dynamic state that is similar to that for supercontinent breakup. Our models do not include such a process for supercontinent breakup.

In our dynamic models on supercontinent formation, we contrast the models with two drastically different convective planforms: small-scale convection and degree-1 convection. An important question is whether degree-1 convection is necessary for supercontinent formation or other long-wavelength convective planforms are equally viable. For example, Evans (2003) proposed that a degree-2 planform with two superplumes similar to the present-day mantle structure is responsible for supercontinent formation with continental blocks merging at the downwelling girdle. Phillips and Bunge (2005, 2007) were able to generate supercontinent cycles in their models with various long-wavelength convective planforms. We believe that answers to this question rely on progress in both modeling long-wavelength mantle convection with tectonic plates and applying them in understanding the observations.

Although in many convection studies (e.g., Bunge et al., 1996; Phillips and Bunge, 2005, 2007; Zhong et al., 2007), the viscosity in the lower mantle is a factor of 30 higher than that for the upper mantle, consistent with inferred from the geoid studies (e.g., Hager and Richards, 1989), significant differences in mantle viscosity exist between these models that could explain the difference in convective planform seen in them. Bunge et al. (1996) and Phillips and Bunge (2005, 2007) did not include temperature-dependent viscosity and used a lithospheric viscosity comparable to the upper mantle viscosity. However, both this study and Zhong et al. (2007) use temperature-dependent viscosity and moderately strong lithosphere (i.e., on average ~200 times stronger than the upper mantle or lithospheric viscosity of 10^{22}–10^{23} Pa s). Zhong et al. (2007) showed that both moderately strong lithosphere and temperature-dependent viscosity may have significant effects on convective planform, consistent with previous studies (Harder, 2000; McNamara and Zhong, 2005).

If the averaged lithospheric viscosity used in Zhong et al. (2007) is reasonable, then degree-1 convection is inevitable, along with supercontinent formation, as indicated in Zhong et al. (2007). The proposed transformation from degree-1 to degree-2 planforms due to circum-supercontinent subduction after supercontinent formation in Zhong et al. (2007) also provides an explanation to present-day mantle structures, particularly the antipodal Pacific and African superplumes. Such a connection between modeled and observed mantle structures in relation to supercontinent processes has not been established in other models (e.g., Phillips and Bunge, 2007). We think that future modeling studies should explore more understanding of present-day mantle structures in the context of supercontinent process.

Unlike Phillips and Bunge (2007) who consider both supercontinent assembly and breakup, our models do not incorporate continental breakup process yet. This is partially due to the different ways of modeling continents. Phillips and Bunge (2005, 2007) used a torque balance method (Gable et al., 1991; King et al., 1992) to model the motion of continents as rigid and un-deformable blocks. While in our modeling, in order to include supercontinent breakup, continental rifting process needs to be considered explicitly as in Gurnis (1998) and Lowman and Jarvis (1995). This may also require modeling nonlinear or plastic deformation of lithosphere at plate margins. This is one of our future research directions.

5. Conclusion

We have investigated processes of supercontinent formation for continental blocks that migrate randomly using a stochastic model and that dynamically interact with mantle convection in dynamic models. Our results can be summarized as follows.

1) Our stochastic modeling calculations suggest that the assembly time of a supercontinent is 1200–1900 Ma based on the averaged speed for the present-day continental motion. This time scale is much longer than ~300–400 Ma for continental assembly inferred for Pangea and Rodinia, suggesting that supercontinent formation is less likely to be a pure random process. However, the assembly time inferred from these stochastic models is sensitive to rules assumed in this type of models which give rise to ~400 Ma supercontinent formation time, as shown in Tao and Jarvis (2002).
2) Our modeling for supercontinent formation with mantle convection focuses on the roles of convective planform. Our results show that continental blocks driven by convection with intrinsically degree-1 thermal structure merge to form a supercontinent in ~250 Ma. During and after supercontinent formation, mantle convection is predominated by a degree-1 planform, consistent with Zhong et al. (2007).
3) Our models with intrinsically short-wavelength thermal structures show that continental blocks may not merge to form a supercontinent, depending on the characteristic wavelengths of mantle flows and the number of continental blocks. In cases when continents merge to form a supercontinent, our modeling shows that the assembly time may be too long and convective wavelengths may be to shorter, compared with observations.

Acknowledgements

This work is supported by the US National Science Foundation and the David and Lucile Packard Foundation.

References

Anderson, D.L., 1982. Hotspots, polar wander, Mesozoic convection and the geoid. Nature, 297, 391–393.
Bercovici, D., 1995. A source-sink model of the generation of plate tectonics from non-Newtonian mantle flow. Journal of Geophysical Research 100, 2013–2030.
Bunge, H.-P., Richards, M.A., Baumgardner, J.R., 1996. The effect of depth-dependent viscosity on the planform of mantle convection. Nature 379, 436–438.
Coltice, N., Bertrand, H., Rey, P., Jourdan, F., Phillips, B.R., Ricard, Y., 2009. Global warming of the mantle beneath continents back to the Archean. Gondwana Research 15, 254–266 (this issue). doi:10.1016/j.gr.2008.10.001.
Eriksson, P.G., Banerjee, S., Nelson, D., Rigby, M., Catuneanu, O., Sarkar, S., Roberts, R.J., Ruban, D., Mtimkulu, M.N., Sunder Raju, P.V., 2009. A Kaapvaal craton debate: Nucleus of an early small supercontinent or affected by an enhanced accretion event? Gondwana Research 15, 354–372 (this issue). doi:10.1016/j.gr.2008.08.001.
Evans, D.A., 2003. True polar wander and supercontinents. Tectonophysics 362, 303–320.
Ernst, W.C., 2009. Archean plate tectonics, rise of Proterozoic supercontinentality and onset of regional, episodic stagnant-lid behaviour. Gondwana Research 15, 243–253 (this issue). doi:10.1016/j.gr.2008.06.010.
Gable, C.W., O'Connell, R.J., Travis, B.J., 1991. Convection in three dimensions with surface plates: generation of toroidal flow. Journal of Geophysical Research 96, 8391–8405.
Gordon, R., Jurdy, D., 1996. Cenozoic global plate motions. Journal of Geophysical Research 91, 12389–12406.
Grand, S.P., 2002. Mantle shear-wave tomography and the fate of subducted slabs. Philosophical Transactions of the Royal Society of London Series A 360, 2475–2491.
Gurnis, M., 1998. Large-scale mantle convection and the aggregation and dispersal of supercontinents. Nature 331, 695–699.
Hager, B.H., Richards, M.A., 1989. Long-wavelength variations in the Earth's geoid: physical models and dynamic implications. Philosophical Transactions of the Royal Society of London Series A 328, 309–327.
Hager, B.H., Clayton, W.R., Richards, M.A., Comer, R.P., Dziewonski, M., 1985. Lower mantle heterogeneity, dynamic topography and the geoid. Nature 313, 541–545.
Harder, H., 2000. Mantle convection and the dynamic geoid of Mars. Geophysical Research Letters 27, 301–304.
Hoffman, P.F., 1991. Did the breakout of Laurentia turn Gondwanaland inside-out? Science 252, 1409–1412.
Honda, S., Yoshida, M., Ootorii, S., Iwase, Y., 2000. The timescales of plume generation caused by continental aggregation. Earth and Planetary Science Letters 176, 31–43.
Jaupart, C., Parson, B., 1985. Convective instabilities in a variable viscosity fluid cooled from above. Physics of the Earth and Planetary Interior 39, 14–32.
King, S.D., Gable, C., Weinstein, S., 1992. Models of convection driven tectonic plates: a comparison of methods and results. Geophysical Journal International 109, 481–487.
Korenaga, J., 2007. Eustasy, supercontinental insulation, and the temporal variability of terrestrial heat flux. Earth and Planetary Science Letters 257, 350–358.
Lenardic, A., Moresi, L.-N., 1999. Some thoughts on the stability of cratonic lithosphere: the effects of buoyancy and viscosity. Journal Geophysical Research 104, 12,747–12,758.
Lenardic, A., Kaula, W.M., 1993. A numerical treatment of geodynamic viscous flow problems involving the advection of material interfaces. Journal Geophysical Research 98, 8243–8260.
Li, Z.X., Evans, D.A.D., Zhang, S., 2004. A 90° spin on Rodinia: possible causal links between the Neoproterozoic supercontinent, superplume, true polar wander and low latitude glaciation. Earth and Planetary Science Letters 220, 409–421.
Li, Z.X., Bogdanova, S.V., Collins, A.S., Davidson, A., Waele, B.D., Ernst, R.E., Fitzsimons, I.C., Fuck, R.A., Gladkochub, D.P., Jacobs, J., Karstrom, K.E., Lu, S., Natapov, L.M., Pease, V., Pisarevsky, S.A., Thrane, K., Vernikovsky, V., 2008. Assembly, configuration, and break-up history of Rodinia: a synthesis. Precambrian Research 160, 179–210.
Lithgow-Bertelloni, C., Richards, M.A., 1998. Dynamics of Cenozoic and Mesozoic plate motions. Reviews in Geophysics 36, 27–78.
Lowman, J.P., Jarvis, G.T., 1993. Mantle convection flow reversals due to continental collisions. Geophysical Research Letters 20, 2087–2090.
Lowman, J.P., Jarvis, G.T., 1995. Mantle convection models of continental collisions and breakup incorporating finite thickness plates. Physics of the Earth and Planetary Interior 88, 53–68.
Maruyama, S., Santosh, M., Zhao, D., 2007. Superplume, supercontinent, and post-perovskite: mantle dynamics and anti-plate tectonics on the Core–Mantle Boundary. Gondwana Research 11, 7–37.
Masters, G., Laske, G., Bolton, H., Dziewonski, A., 2000. The relative behavior of shear velocity, bulk sound speed, and compressional velocity in the mantle: implications for chemical and thermal structure, in Earth's deep interior. In: Karato, S., et al. (Ed.), Mineral Physics and Tomography from the Atomic to the Global Scale. Geophys. Monogr. Ser., vol. 117. AGU, Washington, D.C., pp. 63–87.
McNamara, A.K., Zhong, S., 2004. Thermochemical structures within a spherical mantle: superplumes or piles? Journal Geophysical Research 109, B07402. doi:10.1029/2003JB002847.
McNamara, A.K., Zhong, S., 2005. Degree-one mantle convection: dependence on internal heating and temperature-dependent rheology. Geophysical Research Letters 32 L01301.
Moresi, L.N., Gurnis, M., 1996. Constraints on the lateral strength of slabs from three-dimensional dynamic flow models. Earth and Planetary Science Letters 138, 15–28.
Murphy, B.J., Nance, D.R., Cawood, P.A., 2009. Contrasting modes of supercontinent formation and the conundrum of Pangea. Gondwana Research 15, 408–420 (this issue). doi:10.1016/j.gr.2008.09.005.
Phillips, B.R., Bunge, P.H., 2005. Heterogeneity and time dependence in 3D spherical mantle convection models with continental drift. Earth and Planetary Science Letters 233, 121–135.
Phillips, B.R., Bunge, P.H., 2007. Supercontinent cycles disrupted by strong mantle plumes. Geology 35, 847–850.
Rino, S., Kon, Y., Sato, W., Maruyama, S., Santosh, M., Zhao, D., 2008. The Grenvillian and Pan-African orogens: world's largest orogenies through geologic time, and their implications on the origin of superplume. Gondwana Research 14, 51–72.
Ritsema, H.J., van Heijst, Woodhouse, J.H., 1999. Complex shear wave velocity structure imaged beneath Africa and Iceland. Science 286, 1925–1928.
Rogers, J.J.W., Santosh, M., 2002. Configuration of Columbia, a Mesoproterozoic supercontinent. Gondwana Research 5, 5–22.
Rogers, J.J.W., Santosh, M, 2009. Tectonics and surface effects of the supercontinent Columbia. Gondwana Research 15, 373–380 (this issue). doi:10.1016/j.gr2008.06.008.
Romanowicz, B., Gung, Y.C., 2002. Superplumes from the core–mantle boundary to the lithosphere: implications for heat flux. Science 296, 513–516.
Santosh, M., Maruyama, S., Yamamoto, S., 2009. The making and breaking of supercontinents: Some speculations based on superplumes, super downwelling and the role of tectosphere. Gondwana Research 15, 324–341 (this issue).
Scotese, C.R., 1997. Continental Drift, 7th ed. PALEOMAP Project, Arlington, Texas. 79 pp.
Smith, A.M., Hurley, A.M., Briden, J.C., 1981. Phanerozoic Paleocontinental World Maps. Cambridge University Press.
Solomatov, V.S., 1995. Scaling of temperature- and stress-dependent viscosity convection. Physics of Fluids 7, 266–274.
Su, W.-J., Dziewonski, K., 1997. Simultaneous inversion for 3-D variations in shear and bulk velocity in the mantle. Physics of the Earth and Planetary Interiors 100, 135–156.
Tackley, P.J., 2000. Self-consistent generation of tectonic plates in time-dependent, three-dimensional mantle convection simulations: 1. pseudoplastic yielding. Geochemistry, Geophysics, Geosystems 2000GC000036.
Tao, W., Jarvis, G.T., 2002. The influence of continental surface area on the assembly time for supercontinents. Geophysical Research Letters 29, 40–44.
Torsvik, T., 2003. The Rodinia jigsaw puzzle. Science 300, 1379–1381.
van der Hilst, R.D., 1997. Evidence for deep mantle circulation from global tomography. Nature 386, 578–584.
Veevers, J.J., 2004. Gondwanaland from 650–500 Ma assembly through 320 Ma merger in Pangea to 185–100 Ma breakup: supercontinental tectonics via stratigraphy and radiometric dating. Earth-Science Reviews 68, 1–132.
Weil, A.B., Van der Voo, R., Niocaill, C.M., Meert, J.G., 1998. The Proterozoic supercontinent Rodinia: paleomagnetically derived reconstructions for 1100 to 800 Ma. Earth and Planetary Science Letters 154, 13–24.
Zhao, D., 2009. Multiscale seismic tomography and mantle dynamics. Gondwana Research 15, 297–323 (this issue). doi:10.1016/j.gr.2008.07.003.
Zhong, S.J., Gurnis, M., 1993. Dynamic feedback between an non-subducting raft and thermal convection. Journal Geophysical Research 98, 12219–12232.
Zhong, S.J., Gurnis, M., Moresi, L., 1998. The role of faults, nonlinear rheology, and viscosity structure in generating plates from instantaneous mantle flow models. Journal Geophysical Research 103, 15255–15268.
Zhong, S.J., Zhang, N., Li, Z.X., Roberts, J., 2007. Supercontinent cycles, true polar wander, and very long wavelength mantle convection. Earth and Planetary Science Letters 375, 115–122.
Zhong, S.J., Zuber, M.T., Mories, L.N., Gurnis, M., 2000. Role of temperature dependent viscosity and surface plates in spherical shell models of mantle convection. Journal Geophysical Research 105, 11063–11082.